ELSEVIER

Ceramics International 30 (2004) 977–982

CERAMICS
INTERNATIONAL

www.elsevier.com/locate/ceramint

Microstructure and mechanical properties of Al_2O_3/Ni composites

Guo-jun Li [a,b,*], Rui-ming Ren [a], Xiao-xian Huang [b], Jing-kun Guo [b]

[a] *Department of Materials Science and Engineering, Dalian Railway University, 794 Huanghe Road, Dalian 116028, PR China*
[b] *Shanghai Institute of Ceramics, Chinese Academy of Sciences, Shanghai 200050, PR China*

Received 30 June 2003; received in revised form 16 September 2003; accepted 6 November 2003

Abstract

Ni-coated Al_2O_3 powders were prepared by the heterogeneous precipitation method. After hot-pressing at 1300–1450 °C and 20 MPa, the density of homogeneous Al_2O_3/Ni composites ranges from ∼98% (NA4) to ∼94% (NA8.5) of the theoretical density. Examination by transmission electron microscope (TEM) and scanning electron microscopy (SEM) shows micrometer-size Ni grains to be located at the triple junctions, and with increasing Ni content, the fracture mode of Al_2O_3/Ni composites to change from intergranular mode to transgranular mode due to the thermal stresses. The strength and toughness of composites was much higher than that of the dense monolithic Al_2O_3. The strengthening and toughening mechanisms of the composites with respect to the microstructure are analyzed.

Keywords: A. Powders: chemical preparation; A. Hot-pressing; B. Composites; B. Microstructure-final; C. Mechanical properties; D. Al_2O_3

---

1. Introduction

It is well-accepted that the fracture toughness of the brittle Al_2O_3 ceramic can be increased through the incorporation of ductile metal [1–4]. Reinforcement models also show the importance of the homogeneity and fine size of the metallic inclusions [5]. In general, the control of the microstructure of Al_2O_3/metal composites is very difficult to achieve by traditional techniques involving mechanical mixing of Al_2O_3 and metallic powders followed by hot-pressing. Although a small-scale homogeneity can be obtained using the sol–gel route [6–8], the relatively high cost of some reactants and the difficulty to control the gel drying step are drawbacks of the method.

In recent years, coating as a processing aid for ceramic particles has been investigated. It not only improves the green density and sintered activity [9], but also enhances the uniformity of different phases and mechanical properties of sintered body [10]. However, only few literatures on fabrication of Al_2O_3/metal composite from metal particles coated Al_2O_3 have been reported yet [10]. In the present work, Ni-coated Al_2O_3 powder was first prepared by the heterogeneous precipitation method, and then Al_2O_3/Ni composite was obtained by hot-pressing at appropriate temperature. The densification, microstructure, mechanical properties of the composite were studied.

2. Experimental procedure

Ni-coated Al_2O_3 powders in the desired composition were prepared using Al_2O_3 with average diameter of 0.35 μm (Shanghai Songjiang Fertilizer, Co., China), $Ni(NO_3)_2{\cdot}6H_2O$ (analytically pure) and NH_4HCO_3 (analytically pure) as starting materials. $Ni(NO_3)_2{\cdot}6H_2O$, Al_2O_3 and 0.5 wt.% (equivalent to Al_2O_3 weight) polyacrylic acid as dispersant were firstly mixed in distilled water by ball milling for 48 h. Next, NH_4HCO_3 solution of 1.0 M was added dropwise to the homogeneous slurry obtained above under vigorous stirring. Its reaction was following equation [11]:

$$3Ni^{2+} + 6HCO_3^{-} + H_2O = NiCO_3 \cdot 2Ni(OH)_2 \cdot 2H_2O \downarrow + 5CO_2 \uparrow \quad (1)$$

The precipitates were not dissolved in ammonia solution [12]. To ensure complete reaction, an excess of NH_4HCO_3

---

[*] Corresponding author. Fax: +86-4111-4106828.
E-mail address: guojunlee@163.com (G.-j. Li).

0272-8842/$30.00 © 2003 Elsevier Ltd and Techna Group S.r.l. All rights reserved.
doi:10.1016/j.ceramint.2003.11.004

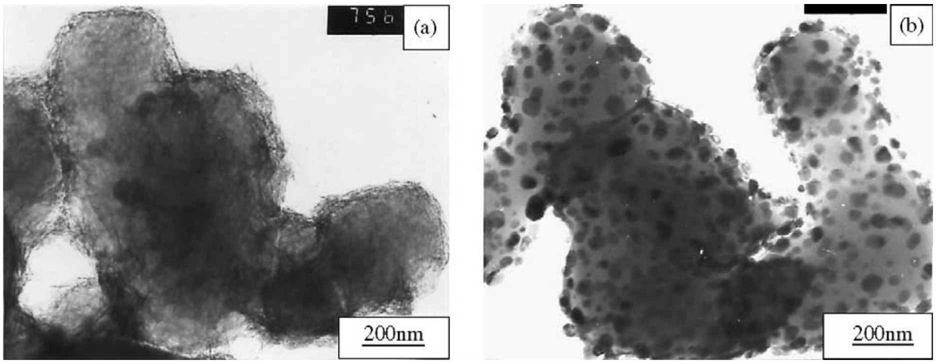

Fig. 1. TEM images of the coated powders (a) the coated powder, (b) as-calcined and reduced powder.

was used and pH value of the mixed solution was adjusted to 8–9 during precipitation. The resulting precipitates were filtered and thoroughly washed with distilled water three times. Finally, the precipitates were washed with ethyl alcohol and dried at room temperature for 24 h. The as-dried precipitates were calcined in air at 550 °C for 2 h, and then the as-calcined powders were reduced at 700 °C for 4 h in hydrogen [13]. The microstructure of the coated powders is shown in Fig. 1. The resulting powders were sintered at 1300–1500 °C for 0.5 h in an argon atmosphere with an applied pressure of 20 MPa. Pure Al_2O_3 ceramic was prepared at 1450–1550 °C for 0.5 h under the same rest conditions as the composite. The sintered bodies were cut to dimensions of 5 mm × 2.5 mm × 30 mm. The samples are designated as NAx, where x is Ni contents.

X-ray diffraction (XRD) patterns were obtained at a scanning rate of 4°/min with 2θ range from 10° to 70° using a fully automated diffraction (Rigaku RAX-10, Japan) with Cu Kα (0.15406 nm) radiation. A transmission electron microscope (TEM) (Model JEM-200CX, JEOL, Tokyo, Japan) was utilized to investigate the particle size, shape of the coated powders and composite. Fracture surfaces were examined by scanning electron microscopy (SEM) (EPMA-8705QHz) to investigate fracture model and grain size. Bulk density was measured by the Archimedes method. Three-point flexural strength measurements were carried out with a span of 20 mm and a crosshead speed of 0.5 mm/min at room temperature by an Instron-1195 Universal Test machine. Fracture toughness, K_{IC}, was determined using an indentation technique with a Vickers indenter (AKASHI) using 98 N load. The formula used for calculating K_{IC} was expressed as $K_{IC} = A(E/H)^{1/2}(p/c^{2/3})$ [14]. A minimum of six specimens was tested to obtain a signal datum.

3. Results and discussion

3.1. Densification

Fig. 2 is the variation of relative densities for Al_2O_3/Ni composites containing different Ni content with hot-pressing temperature. The relative density of the samples enhances with increasing sintering temperature. When Ni content is relatively lower (for example NA4, NA6.5), the samples attain the highest relative densities of 98.6% at 1450 °C. In contrast to monolithic Al_2O_3 ceramic with the same density, sintering temperature decreases by about 100 °C. It can be seen from Fig. 3 that there are lot of pores in sintered sample at 1450 °C, and few in sintered sample at 1550 °C. The reason is that Ni particles (∼20 nm) in the coating layer are very fine, and the activity of sintering is largely enhanced. When Ni content is relatively higher (for example NA8.5), the samples attain the highest relative densities of ∼94% at 1400 °C. Above 1400 °C, the relative density of the samples containing high Ni content is lower than that of the samples containing low Ni content. Al_2O_3 is not wetted by solid or liquid Ni [7,15]and the thermal expansion coefficient of Ni ($15 \times 10^{-6}\,°C^{-1}$) is larger than that of Al_2O_3 ($8.4 \times 10^{-6}\,°C^{-1}$), so the sintered samples produce more pores at the interface of Al_2O_3/Ni (see Fig. 4) when the composites are cooled down from a sintering temperature. The more Ni content is high the more the interface of Al_2O_3/Ni is big, and then the more the produced pores are many (Fig. 4b). This phenomenon can be observed from Fig. 5. As a result, the relative density of the samples containing high Ni content is relatively lower.

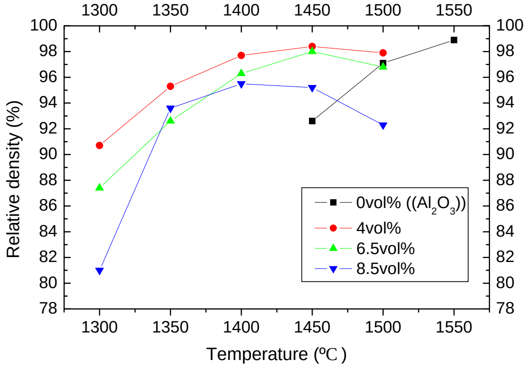

Fig. 2. Relative densities vs. sintering temperature for Al_2O_3/Ni composite by hot-pressing.

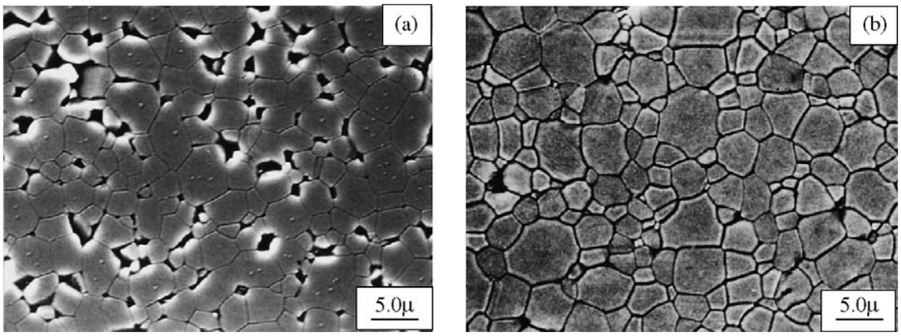

Fig. 3. Thermally etched photos of the pure Al_2O_3. (a) 1450 °C, (b)1550 °C.

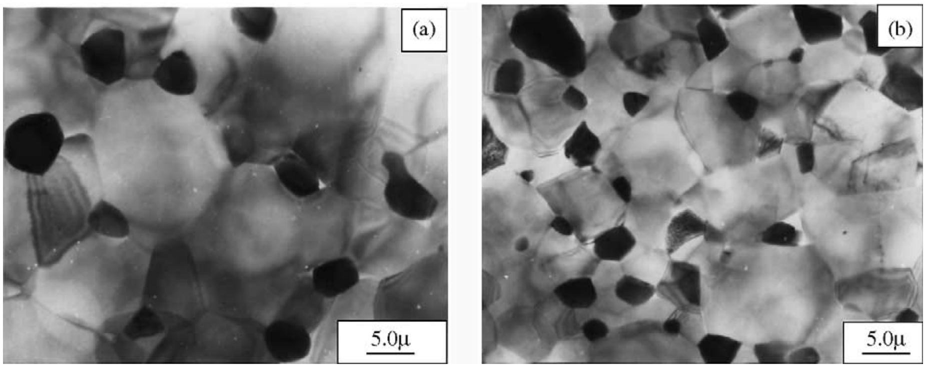

Fig. 4. TEM micrographs of the sample obtained at 1450 °C, (a) NA4, (b) NA8.5.

3.2. Microstructure

Fig. 5 is thermally etched photos of the Al_2O_3/Ni composites containing different Ni contents. The grain structure of matrix phase and inclusion are noted. Because the atomic number of Ni is far higher than Al_2O_3, the scattering contrast results in a white feature for Ni grains and gray for Al_2O_3 grains. The micrographs clearly reveal that Ni grains are agglomerated, located at the triple junctions, and homogeneously dispersed in Al_2O_3 matrix. On the other hand, some exaggerated Al_2O_3 are found. However, TEM (Fig. 6) indicates some small Ni particles of less than 0.3 μm exist in the exaggerated Al_2O_3. In an early stage of sintering, the separation between grain boundary and small inclusions can take place as the velocity of grain boundary is much faster than that of inclusions, therefore, small Ni particles can be swallowed in the matrix grains during matrix grain growth [16,17]. The Ni entrapped in Al_2O_3 matrix can refine matrix grains.

The average size of Al_2O_3 and Ni grains are given in Table 1 by calculating and measuring (see Figs. 3 and 5). The average grain size of monolithic Al_2O_3 is much bigger

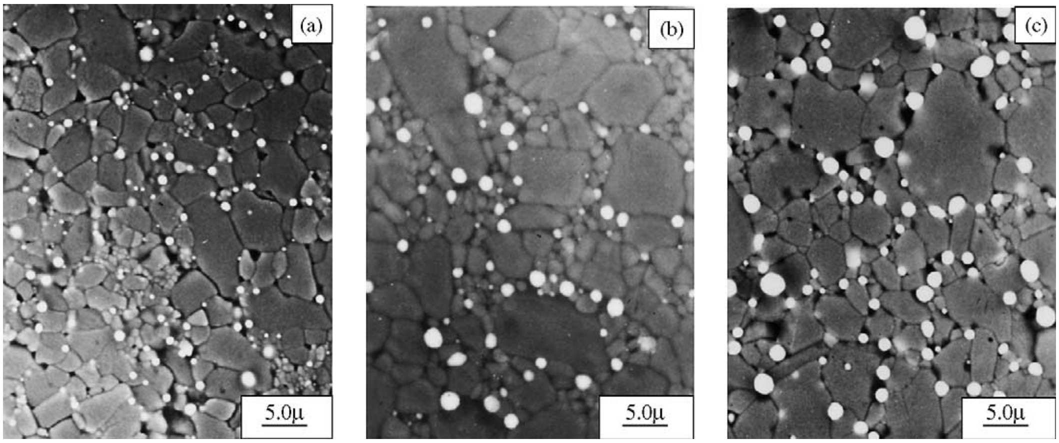

Fig. 5. Thermally etched photos of the Al_2O_3/Ni composites. The nickel content in the composites is (a) 4, (b) 6.5, (c) 8.5.

Table 1
The average size of Al_2O_3 and Ni particles calculated by the linear intercept method and statistical method

Samples	Hot-pressing temperature (°C)	Holding time (h)	Ni grain size (μm)	Al_2O_3 grain size (μm)
NA0	1450	0.5		~2.0
NA0	1550	0.5		~2.5
NA4	1450	0.5	0.44	~1.2
NA6.5	1450	0.5	0.51	~1.3
NA8.5	1450	0.5	0.84	~1.5

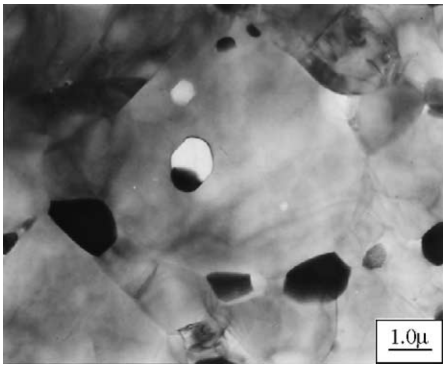

Fig. 6. Typical micrographs of the exaggerated Al_2O_3 matrix grins.

than that of Al_2O_3/Ni composites, which shows that the introduction of Ni particles can restrain the growth of Al_2O_3 grains. However, with increasing Ni content, the average size of Ni and Al_2O_3 grains become big, namely, effect on restraining the growth of Al_2O_3 grains becomes weak. This may qualitatively be explained by Zener's model [18].

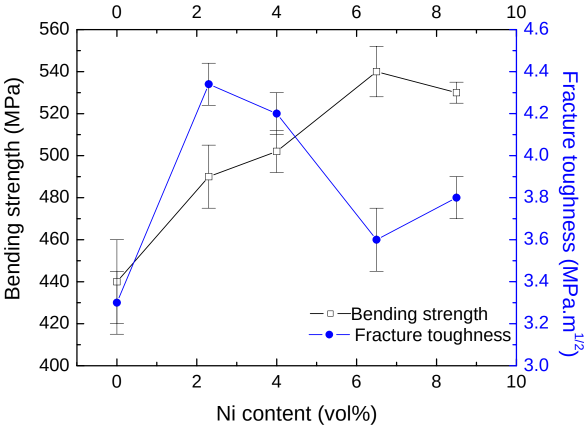

Fig. 8. Relation of bending strength, fracture toughness and Ni content.

According to Zener's model, the ultimate grain size of the matrix (***G***) is expressed as the following equation:

$$\boldsymbol{G} = \frac{4r}{3f} \tag{2}$$

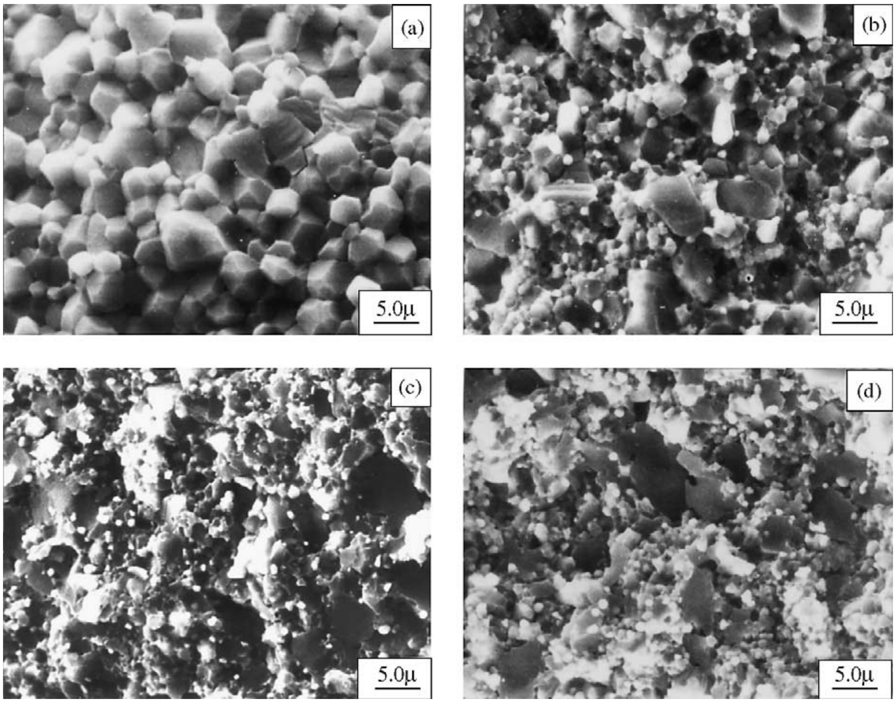

Fig. 7. SEM micrographs of fracture surface of the samples with different Ni content (a) Al_2O_3, (b) NA4, (c) NA6.5, (d) NA8.5.

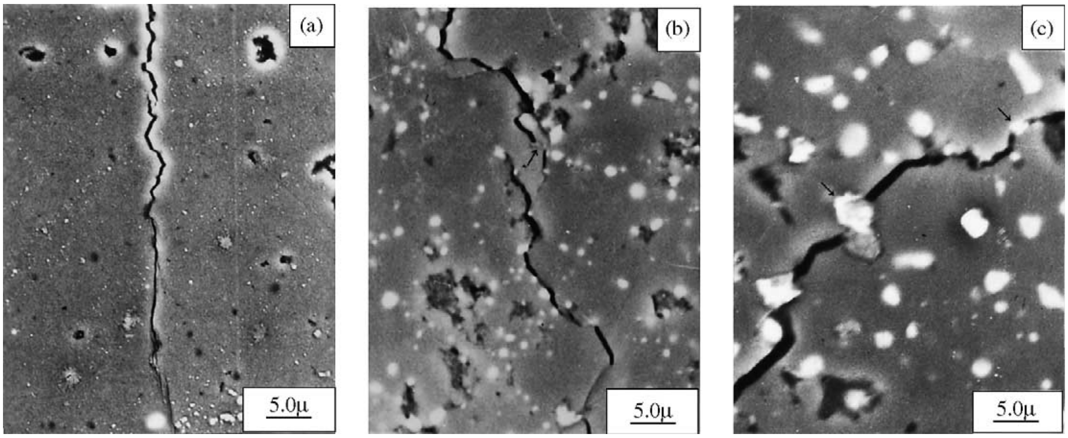

Fig. 9. SEM micrographs showing the crack propagation from the polished surface of samples (a) Al_2O_3, (b) NA4, (c) NA8.5.

where r and f are grain diameter and volume fraction of the second phase, respectively. Zener's model indicates that when grain diameter of the second phase is constant, the grain size of the matrix decreases with increasing volume fraction of the second phase. Thus, the introduction of Ni particles can restrain the growth of Al_2O_3 grains. And when f is constant, the grain size of the matrix becomes big with increasing the size of second phase. In this paper, with increasing Ni content, nanoNi grains agglomerated and grown during sintering. Therefore, effect on restraining the growth of Al_2O_3 grains becomes weak.

Fig. 7 is SEM micrographs of fracture surface of the samples with different Ni content. It can be observed that the fracture mode of monolithic Al_2O_3 is basically intergranular fracture, and the fracture model changes from intergranular model to transgranular model as Ni content is enhanced. The change in fracture mode can be explained on the basis of thermal stresses. When the composite is cooled down from a sintering temperature, the thermal stresses are generated in the composite produce due to thermal coefficient mismatch between the ceramic matrix and inclusions. Since the thermal expansion coefficient of Ni ($15 \times 10^{-6}\,{}^\circ C^{-1}$) is larger than that of Al_2O_3 ($8.4 \times 10^{-6}\,{}^\circ C^{-1}$), according to the theory proposed by Selsing [19], a radial tensile stress and tangential compressive stress are produced in Al_2O_3 matrix. For this reason, the interface of Al_2O_3/Al_2O_3 and the inner of Al_2O_3 are subjected to a compressive stress and a tensile stress, respectively. This strengthens the interface of Al_2O_3/Al_2O_3 and weakens Al_2O_3 matrix resulting in transgranular fracture. In addition, Taya et al. [20] indicate the thermal stresses in the matrix is proportional to the amount of inclusions. Thus, with increasing Ni content, the fracture mode of Al_2O_3/Ni composites changes from intergranular mode to transgranular model.

3.3. Mechanical properties

The strength and the toughness of the composites are shown as a function of Ni content in Fig. 8. Each point in the figures represents the average value of four specimens. The error bars indicate one standard deviation. Compared with the dense monolithic Al_2O_3, Al_2O_3/Ni composites show a marked increment in both strength and toughness. For example for NA4 sample, the strength and the toughness increase by 15–28%, respectively.

According to Griffith theory, the fracture strength (σ_f) of brittle material is expressed as the following equation:

$$\sigma_f = \left(\frac{1}{Y}\right)\frac{K_{IC}}{c^{1/2}} \tag{3}$$

where K_{IC}, c and Y are the fracture toughness, one-half the width of the initial flaw and the geometrical parameter of a flaw, respectively. In general, c is proportional to the grain size (d) in dense polycrystalline materials. Thus, the fracture strength increases when the grain size is small (Eq. (3)). Therefore, the higher strength of the Al_2O_3/Ni composite is attributed to the decrease in grain size of the Al_2O_3 matrix (see Table 1). When Ni content is higher, the decrease in the strength of the composites results from the decrease of the density of the composites [21].

Fig. 9 is SEM micrograph showing the crack propagation from the polished surface of the composite. Except for the crack deflection toughening, the crack branching and crack bridging (arrow) are contributed to the increment of the fracture toughness.

4. Conclusions

NanoNi coated Al_2O_3 composite powders were successfully synthesized by the heterogeneous precipitation method via using Al_2O_3, $Ni(NO_3)_2 \cdot 6H_2O$ and NH_4HCO_3 as starting materials, subsequently, which were sintered by hot-pressing at 1300–1500 °C for 0.5 h to obtain Al_2O_3/Ni composites. The density of the composites was found to range from ∼98% (NA4) to ∼94% (NA8.5) of the theoretical density.

Microstructure studies found that Ni grains are agglomerated, located at the triple junctions, and homogeneously dispersed in Al_2O_3 matrix. With increasing Ni content, the fracture mode of Al_2O_3/Ni composites changes from intergranular model to transgranular mode due to the thermal stresses.

In contrast to the dense monolithic Al_2O_3, the addition of nanoNi can reduces sintering temperature, decreases in grain size of Al_2O_3 matrix, and shows a marked increment in the mechanical properties. The increment of strength is due to microstructural refinement. Toughness enhancement is attributed to crack deflection, crack branching and crack bridging.

References

[1] W.H. Tuan, R.J. Brook, The toughening of alumina with nickel inclusions, J. Eur. Ceram. Soc. 6 (1990) 31–37.

[2] T. Sekino, K. Niihara, Fabrication and mechanical properties of fine-tungenten-dispersed alumina-based composites, J. Mater. Sci. 32 (1997) 3943–3949.

[3] S.A. Cho, M. Puerta, B. Cols, J.C. Ohep, Sintering behavior of Al_2O_3–Cr and Al_2O_3–Cr$(NO_3)_3$ mixtures, Powder Metall. Int. 12 (1980) 192–195.

[4] S.T. Oh, T. Sekino, K. Niihara, Fabrication and mechanical properties of 5 vol% copper dispersed alumina nanocomposite, J. Eur. Ceram. Soc. 18 (1998) 31–37.

[5] A.G. Evans, High toughness ceramics, Mater. Sci. Eng. A 105/106 (1988) 65–75.

[6] E. Breval, G. Dodds, C.G. Pantano, Properties and microstructure of Ni–alumina composite materials prepared by the sol/gel method, Mater. Res. Bull. 20 (1985) 1191–1205.

[7] E. Breval, Z. Deng, et al., Sol–gel prepared Ni–alumina composite materials, Part I. Microstructure and mechanical properties, J. Mater. Sci. 27 (1992) 1464–1468.

[8] E.D. Rodeghiero, O.K. Tse, J. Chisaki, E.P. Giannelis, Synthesis and properties of Ni–α-Al_2O_3 composites via sol–gel, Mater. Sci. Eng. A 195 (1995) 151–161.

[9] C.M. Wang, F.L. Riley, Alumina-coating of silicon nitride powders, J. Eur. Ceram. Soc. 10 (1992) 82–93.

[10] W.H. Tuan, H.H. Wu, T.J. Yang, The preparation of Al_2O_3/Ni composites by a powder coating technique, J. Mater. Sci. 30 (1995) 855–859.

[11] Y. Li, C. Li, X. Duan, et al., Preparation of nanocrystalline NiO in mixed solvent, J. Chin. Univ. Sci. Technol. 27 (3) (1997) 346–349.

[12] J.A. Dean, Lange's Handbook of Chemistry, 13th ed., McGraw-Hill Book Company, 1985.

[13] G.-J. Li, X.-X. Huang, J.-K. Guo, Fabrication of Ni-coated Al_2O_3 powders by the heterogeneous precipitation method, Mater. Res. Bull. 36 (2001) 1307–1315.

[14] G.R. Anstb, P. Chantikul, B.R. Lawn, D.B. Marshall, A critical evaluation of indentation techniques for measuring fracture toughness: I, direct crack measurements, J. Am. Ceram. Soc. 64 (1981) 533–538.

[15] W.H. Tuan, R.J. Brook, Processing of alumina/nickel composites, J. Eur. Ceram. Soc. 10 (1992) 95–100.

[16] H.Z. Chen, W.H. Tuan, Pressureless sintering of Al_2O_3/Ni nanocomposites, J. Eur. Ceram. Soc. 19 (1999) 463–468.

[17] T. Sekino, T. Nakajima, S. Ueda, K. Niihara, Reduction and sintering of a nickel-dispersed-alumina composite and its properties, J. Am. Ceram. Soc. 80 (1997) 1139–1148.

[18] C. Zener, Trans. Am. Inst. Mining Metall. Eng. 175 (1948) 48 (as communicated by C.S. Smith).

[19] J. Selsing, Internal stresses in ceramics, J. Am. Ceram. Soc. 44 (8) (1961) 419–419.

[20] M. Taya, S. Hayashi, S. Kobayashi, H.S. Yoon, Toughening of a particulate-reinforced ceramic-matrix composite by thermal residual stress, J. Am. Ceram. Soc. 73 (5) (1990) 1382–1391.

[21] S.C. Wang, W.C.J. Wei, Characterization of Al_2O_3 composites with Mo particulates, II. Densification and mechanical properties, Nanostruct. Mater. 10 (1998) 983–1000.